Mechanics and Mechanical Engineering
Vol. 18, No. 1 (2014) 53–71


# The Viscoplastic Effect in the Heat–Treated, Thin–Walled AL–6060 Alloy Profiles Subjected to Compressive Axial Impact

Andrzej Mróz
*Faculty of Mechanical Engineering*
*Lodz University of Technology*
*Stefanowskiego 1/15, 90–924 Łódź, Poland*
*andrzej.mroz.pl@gmail.com*

Received (11 August 2014)
Revised (16 September 2014)
Accepted (29 September 2014)

This paper will highlight the influence of the strain rate effect occurring during pulse loading on dynamic stability of aluminium profiles. Current work is the development of the analysis carried in [1]. The C–channel cross–section beams/columns are made of 6060 T4, T5, T6 and T66 aluminium alloy. The rectangular–shape compressing pulse is analysed. The static material characteristics had been obtained from the experimental tensile tests and afterwards modified for dynamic response according to Perzyna viscoplastic model. The results of the numerical computations are presented whereas the critical load and DLF (Dynamic Load Factor) basing on the selected dynamic buckling criterion is determined.

*Keywords*: Perzyna model, aluminium aging, thin–walled profiles, dynamic stability analysis, dynamic buckling criterions.

## 1. Introduction

Among the vast diversity of manufacturing technologies, the significant part of them bases on the material flow processing, in particular: extrusion, bending, stretching, casting and rolling (presented in Fig. 1). For this reason, material science has been searching for the realistic material characteristic in elasto–plastic range for over the century.

The first attempts to describe the material characteristic in elasto–plastic range were carried by Andrade [2], who proposed the plastic–flow formulations. The complex analysis of the stability of thin walled structures in elasto–plastic range (with bilinear, multilinear, Ramberg–Osgood theory descriptions), under static loads have been carried out by M. Królak et al. in [3] and [4] for isotropic and orthotropic materials respectively. Orthotropic plates subjected to axial compression were considered by K. Kowal–Michalska [5] where the Hill yield criterion and Prandtl–Reuss equations have been implemented to describe the flow effect.

Some of the manufacturing processes including aluminium implementation have been investigated in the frame of thermal–elasto–plastic rules. The influence of the bearing area parameters on the extruded aluminium profiles is analysed in [6]. The two types of material flow are considered- with and without contact, which is crucial for the final quality of extrusion. The viscoplasticity effect in the elevated temperatures and the influence of heat treatment (aging) on the yield stress evolution of the 319 foundry aluminium alloy was presented by Martinez, Russier, Couzinie, Guillot and Cailletaud [7]. The hot rolling simulation of AA5083 aluminium alloy using Finite Element Method, basing on thermo–viscoplastic material behaviour is described by Shahani, Nodamaie and Salehinia [8].


**Figure 1** Aluminium profile: extrusion (a), bending (b) and stretching (c) (A. Mróz photo)

## 2. Viscoplasticity

Most of the available engineering materials, which are considered in scientific research are analysed in elastic range for low strain and described by simplified Hooke's law, where the stress $\sigma$ is proportional to strain $\varepsilon$ by Young's Modulus $E$. This relation corresponds to the ideal state in elastic range. In fact, due to dynamic load or time–dependant effect, almost all materials exhibit deviation in various: either the elastic or viscous characteristics which are evident in over yield range. As a consequence of this discrepancy, the sciences: rheology and plasticity have been developed, in fact actually apart from each other.

When it comes to rheology, the plasticity effect is considerably neglected as having no or minor influence on material characteristic. On the other hand, when focusing only on plasticity effect, short duration loading and quasi–static response is analysed, omitting creep or relaxation phenomenon. For this reason, firmly bridging view has been adopted: the viscoplasticity.

The above theory was developed by Hohenemser and Prager [9]. Thereafter, several viscoplastic models have been universally developed and adopted. The most common ones are Perzyna [10], [11], Duvaut–Lions [12] and Wang models [13], [14]. This paper will focus on the Perzyna viscoplasticity overstress model application.

Nowadays, two major viscoplastic, rate dependent overstress models have been universally developed the Perzyna and the Duvaut–Lions models. When it comes to Perzyna, in initial assumption the direction of viscoplastic flow was determined by the gradient of a plastic potential function calculated at the current stress point.

The Perzyna constitutive model is noted in Eqn. (1).

$$\sigma = \left[1 + \left(\frac{\dot{\varepsilon_{pl}}}{\gamma}\right)^m\right]\sigma_0(\varepsilon_{pl}) \tag{1}$$

In this equation, $\sigma$ is the stress, expressed as a function of plastic strain rate, $(\varepsilon_{pl})$, material viscosity parameter $\gamma$, strain rate hardening parameter, $m$, and the static subsequent yield stress, $\sigma_0$.

Since its formulation by Perzyna in 1963, viscoplasticity theory has been fairly developed. Although Perzyna's model is commonly associated with the definition of viscoplastic strain rates in terms of overstress function only, it presents the form that belongs to the most general and elegant formulation in mechanics and includes: invariance with respect to any diffeomorphism (covariant material model), well–posedness of evolution problem, sensitivity to the rate of deformation, finite elasto–viscoplastic deformations, plastic non–normality, dissipation effects (anisotropic description of damage), thermo–mechanical couplings and length scale sensitivity. On the other hand, it is important that the viscoplasticity theory, being a physical one, has a deep physical interpretation derived from the analysis of a single crystal and/or polycrislal behaviours. It is clear that the theory of Perzyna's type viscoplasticity, in its current form, belongs to one of the most complex constitutive models. It is a consequence of the results which showed that for robust modelling the number of important phenomena included in the description must be high. Hence, the number of material parameters in the model is considerable and the model calibration needs nonstandard methods. Thus, very detailed experimental examination of a particular material, under vast range of strain rates, temperatures and scales of observations is needed [15].

## 3. Dynamic stability of thin–walled, visco–plastic structures

The primary methods on experimental determination of metal dynamic characteristics and comparison to analytical models have been published in [16], [17] and [18]. In their publication Gilat and Wu, who tested rolled, steel specimen in elevated temperatures confirmed the significant influence of strain rate on material aging effect and concluded, that it is impossible to describe the material characteristic with single constitutive equation in complete strain rate range. Some remarks on friction stir welding, which is the modern way of joining the metal members were described in [19].

Although the amount of publications regarding the numerical calculations of viscoplastic behaviour of materials is numerous, most of them are directed on technological processing and applications. Those devoted to dynamic stability of thin walled structures, generally contain shell [20], [21], [22] and plated structures analysis [23], [1].

This paper focuses on a plate type member, includes dynamic stability considerations and analysis of the viscoplasticity effect defined by the Perzyna analytical equation. It is important to mention, that the results of the computations should be validated by experimental tests.

Due to the fact that the response of the structures depends on a type of applied loading, static, quasi–static and dynamic stability criteria were assigned. In the literature resources, only a few positions are devoted to the influence of strain–rate effect on dynamic stability, although this phenomenon is ubiquitous e.g. manufacturing processes (punching, notching, form–pressing) and applications (automotive energy absorbers).

For this reason, the author decided to analyse the general case of dynamic stability of heat–treated, simply supported aluminium C–channel profile, subjected to axial impulse loading. The pulse duration was equal to the period of fundamental natural flexural vibrations. The material characteristics, which were achieved from own static experimental tests, were modified by Perzyna equations and are presented in Fig. 4. The detailed analysis' steps are described in paragraph 5: *Formulation of the problem.*

## 4. Determination of material constants

The literature resources referring to aluminium viscoplasticity is very poor, however a position of T. Mukai, K. Ishikawa and K. Higashi should be highlighted [24]. In their paper, the authors carried out extensive research on the influence of strain rate on the mechanical properties of various, different graded aluminium alloys. It is evident that for almost all alloys the increase of yield stress is observed. In some kinds of solution-strengthening materials, such as A1-Mg system alloys, the negative strain rate sensitivity of flow stress has been reported whereas the increase in yield stress occurred. The source of this phenomenon is explained by dynamic strain aging for low and damping mechanisms at high strain rates. Al6060 is a type of Al–Mg–Si alloy. The stress – strain curves for IN905XL aluminium alloy are presented in Fig. 2.

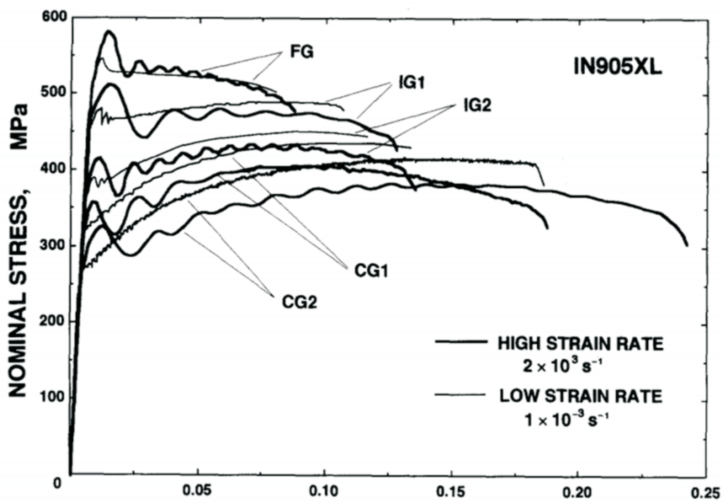


**Figure 2** Typical stress–strain curves for IN905XL aluminum alloy with five different grain sizes [24]

Due to the lack of experimental feedback, the strain–rate parameters $m$ and $\gamma$ noted in the Perzyna equation (1) were determined basing on available characteristics, achieved by the cited authors. For this, the curve fitting method was employed. In the case of modification the low strain rate characteristic (which was equivalent to the static tensile curves), the selected parameters, $m$ and $\gamma$, were matched so that the material characteristic runs were fairly compatible with dynamic test results for high strain rate. In this article the high strain rate is analysed. For the $m = 0.24$ and $\gamma = 9$ good consistence appears (Fig. 3).

These parameters were used to modify the static tensile curves. The characteristics of 6060 aged tempers and modified by Perzyna equations are presented in Fig. 4. Additionally, the process was isothermal and for this reason the parameters $m$ and $\gamma$ were constant.

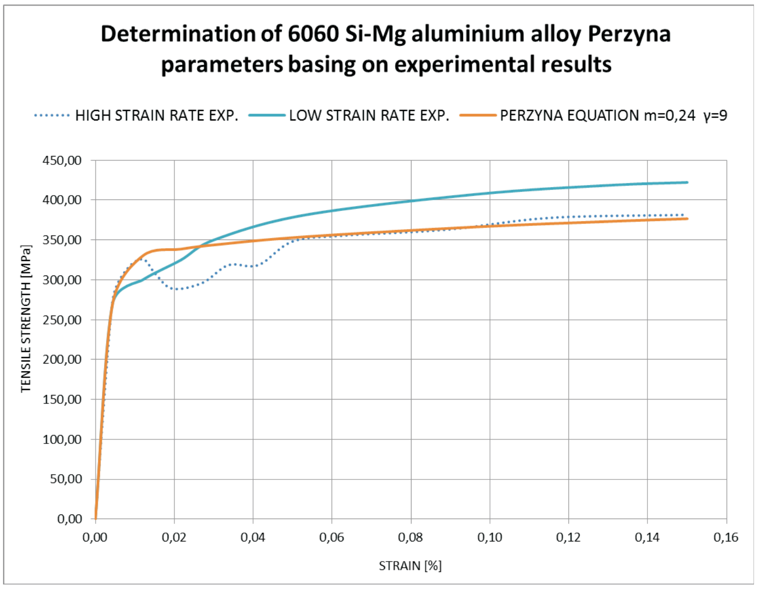


**Figure 3** Determination of Perzyna constants basing on experimental results achieved according to [24]

## 5. Dynamic stability criterions

The dynamic buckling occurs in the structure, when a sudden pulse load of intermediate amplitude and duration close to the period of fundamental natural flexural vibrations is applied to the model. The analysis can be multistage, the shape (rectangular, sinusoidal, triangular, multistep), time duration and amplitude can be modified [25]. It is noticeable, that when the time duration of the pulse is too long, the response of the structure may become quasi–dynamic. This effect was analysed in [26].

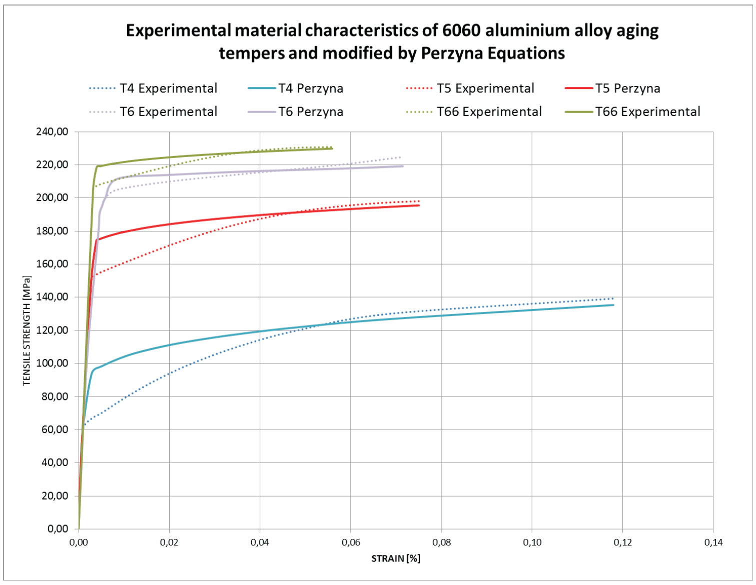


**Figure 4** Material characteristics of 6060 aluminium alloy aging tempers from static tensile tests modified by Perzyna Model

The dynamic buckling of the thin–walled structures and applicable criterion have been developed as the years have been passing, but still there is discussion about the most accurate one when determining the critical stress: Budiansky–Hutchinson [27], Ari Gur and Elishakov [28], Volmir, Petry–Fahlbush, Ari Gur and Simonetta [29], Kubiak [30]. To mention, Budiansky–Hutchinson [31] as well as other authors [25], introduced Dynamic Load Factor which is a quotient of dynamic pulse magnitude $\sigma_{z\,imp.}$ and static buckling load $\sigma_{cr}$:

$$DLF = \frac{\sigma_{z\,imp.}}{\sigma_{cr}} \tag{2}$$

In the current paper the below mentioned criteria have been used:

1) Budiansky–Hutchinson criterion [30]

*Dynamic stability loss occurs when the maximum deflection grows rapidly with the small variation of the load amplitude.*

2) Petry–Fahlush criterion [32]

*A dynamic response caused by a pulse load is defined to be dynamic stable if the condition that the effective stress is not greater than defined limit stress is fulfilled at every time and everywhere in the structure.*

3) Volmir criterion [29]

*The dynamic critical load corresponds to the amplitude of pulse load (of constant duration) at which the maximal plate deflection is equal to some constant value k (e.g. one plate thickness).*

## 6. Formulation of the problem

The profiles under considerations were made of isotropic material – 6060 aluminium alloy aged in T4, T5, T6 and T66 tempers. For numerical computations it was assumed that the analysed profile is of 600 mm length and its flanges are of 30 mm wide, a web is of 80 mm wide where the wall thicknesses of both are equal to 1 mm. The geometrical cross-section dimensions are presented in Fig. 5.

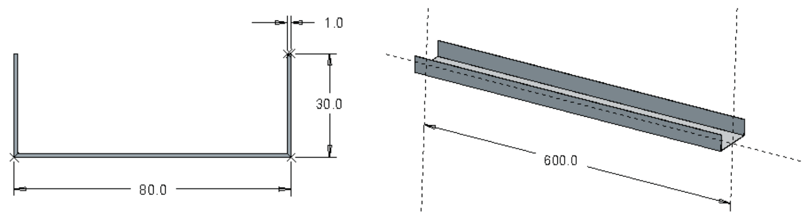


**Figure 5** The geometrical cross–sectional dimensions of analyzed C–shape Profile

The boundary conditions which followed the analytical assumption of simply supported loaded profile edges were obtained through properly constrained displacements of these FEM model edges (Fig. 6). To fulfil the condition of profile edges being rectilinear additional coupling constrains were introduced (see Fig. 8b). Therefore, all these displacement constrains allowed replication of beam/column/girder edge behaviour from classical mechanics of materials approach.

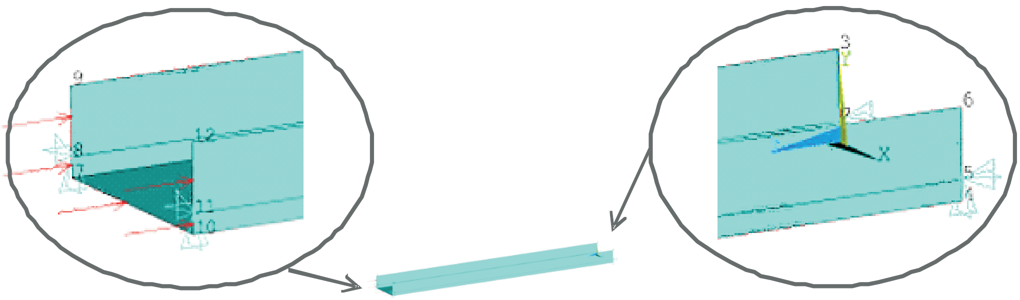

**Figure 6** Load and supporting mode of the analyzed profile

The solution included the analysis of the postbuckling response of the structure, also when the load was removed after the pulse in the period range ($T_{imp.} - 2\,T_{imp.}$). Graphically this is presented in Fig. 7. Zero initial conditions were assumed for initial velocity and displacement.

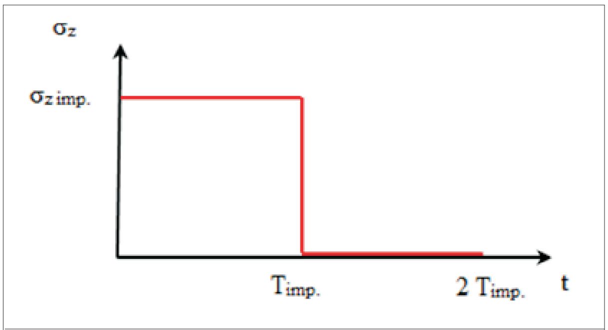


| | |
|---|---|
| For $0 \leq t \leq T_{imp}$ | $\sigma_z = \sigma_{z\ imp}$ |
| For $t \geq T_{imp}$ | $\sigma_z = 0$ |

**Figure 7** The rectangular impulse loading characteristics

## 7. Results of numerical analysis

### 7.1. *Finite Element Method model*

In this work the main interest was a transient analysis which allowed modelling a dynamic response of the structure. It was preceded by linear buckling analysis and modal analysis. From the first one, the critical load was determined as well as the first buckling mode. During the modal analysis the period of natural flexural vibrations were established. Among them a value was adopted as reference for pulse duration.

The finite element method (FEM) was used for nonlinear simulation of the dynamic buckling interaction behaviour of the open cross-section profiles, subjected to a pulse compression. Following the ANSYS Guide [33], the element SHELL 181 type (Fig. 8a) is strongly recommended for the thin–walled structures with large strain and was used for model discretization. The total number of elements exceeded 1000 (Fig. 8b).

The element has four nodes and six degrees of freedom at each node: translations in the $x$, $y$, and $z$ directions, and rotations about the $x$, $y$, and $z$ axes. The SHELL181 is associated with shell section option which is more general method to define a cross–section, especially for the multi–layered constructions.

The boundary conditions which followed the analytical assumption of simply supported loaded profile edges were obtained through properly constrained displacements of these FEM model edges. To fulfil the condition of profile edges being rectilinear additional coupling constrains were introduced (Fig. 8b). Therefore, all these displacement constrains allowed replication of beam/column/girder edge behaviour from classical mechanics of materials approach. Taking into considerations assumptions presented in paragraph [3], the time duration was limited to 1.0 to the period of fundamental natural flexural vibrations, which was formerly determined in the modal analysis. The modal form (8–th set) was compared to corresponding static buckling mode, achieved by Eigen- buckling analysis (presented in Fig. 9), consequently the pulse duration was defined as 1,72ms.

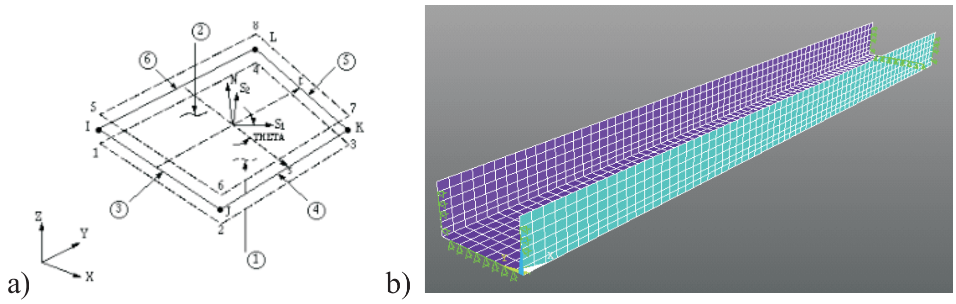


**Figure 8** Element type Shell 181 (a) and discretized FEM model with BC (b)

The numerical analysis was three–staged:

1) Modal analysis and mode forms (10 sets)

2) Eigen–Buckling analysis (5 modes)

*The Eigenvalue buckling analysis is a method to determine the critical load and buckling form for elastic structures. This option is of a conservative imperfection and is applied to geometrically ideal structures. In fact, the constructions tend to fail under lower buckling loads due to the real structural imperfections. Critical stress for T4, T5. T6 and T66 equals 38.6, 38.4, 38.4, 38.3 [MPa] respectively.*

*In this step of analysis, the characteristic node 2779 (corresponding to maximum transverse deflection) was determined in order to verify the failure mode of the profile. The location and critical buckling load is presented in Fig. 10.*

3) Transient analysis *The analysis included 2 load steps, corresponding to course in Fig. 7. Each load step was divided into 200 sub–steps, which were optimized for computer effectiveness and acceptable result accuracy.*

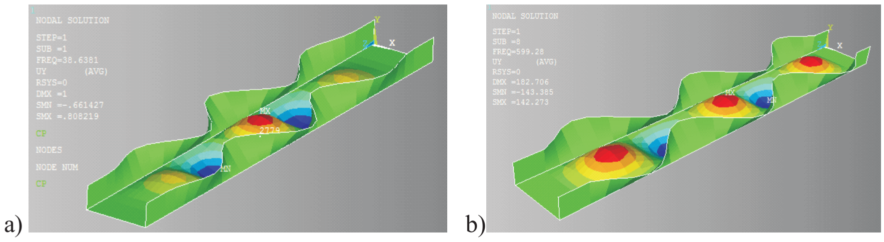

**Figure 9** Eigen buckling mode (a) and modal mode (b) comparison (8-th set of modal analysis)

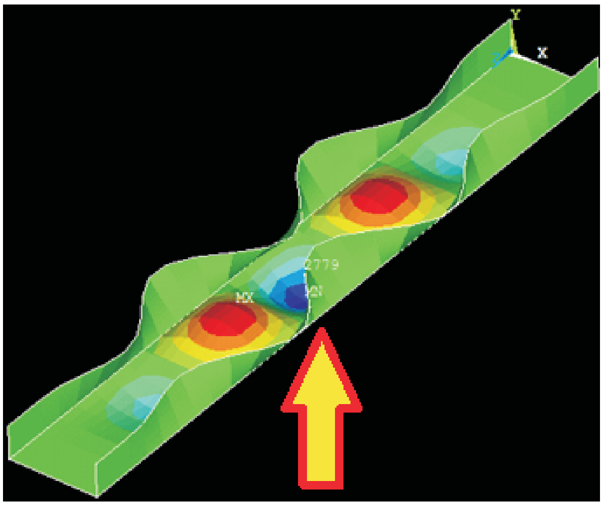


**Figure 10** Location of characteristic node, the vertical deflection and critical buckling load achieved by Eigen Buckling Analysis

Some parameters were analysed when loading the profile:

1. *UY deflection of the reference node 2779 and characteristic instant corresponding to the first amplitude in displacement route (Fig. 11).*
2. *Von–Misses Stress in the characteristic instant for the whole member.*
3. *Maximum UY deflection (and node ID) in the characteristic instant and compared to reference node 2779.*

The data achieved in this way was used to determine the critical dynamic buckling load, basing on cited criterion in chapter 3. The results were compared to the achieved solutions for dynamic stability analysis for experimental material characteristics in the previous author's paper [1].

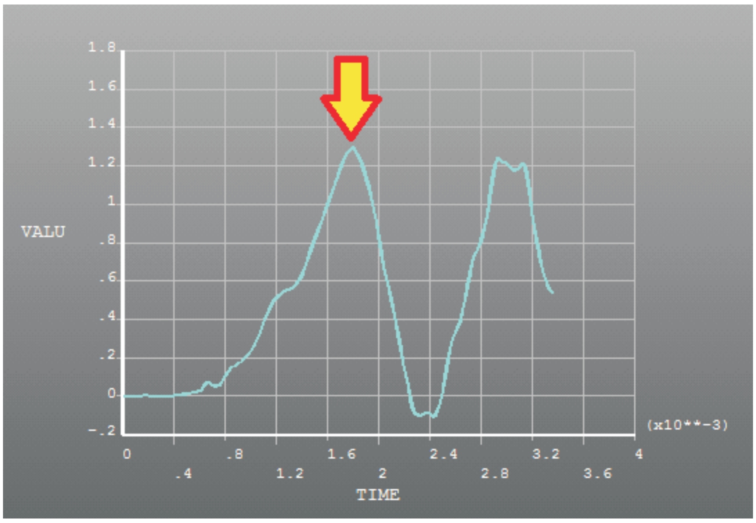


**Figure 11** Spatial displacement route for selected node

## 8. Results of computations

The experimental static material characteristics modified by Perzyna equation (Fig. 4), are characterised by elevated yield stress and decreased course in the hardening range. The influence of this change, in comparison to the original static tensile results is analysed in current subsection. The computations are performed in compliance with the procedure, proposed by the author, described thoroughly in [1].

The UY translation curves of the specific node 2779 are presented in (Fig. 12). This node was selected due maximum UY displacement in eigen–buckling analysis. The location of characteristic node is presented in Fig. 10. The analysis is carried for all aging tempers T4T66. In the low DLF range (0.8–1.1) no significant difference was observed in the dynamic response of the structure. From the DLF equal to 1.2, a steady growth of UY deflection appeared for the T4–T6. For these members, according to Budiansky–Hutchinson this was the critical dynamic load. The T66 structure tended to steady deflection growth was until the DLF value of 1.4 when the deflection increased and was equal to wall thickness of the profile.

For the needs of the Volmir criterion (a critical deflection assumed equal to the wall thickness) the straight line on the Fig. 12 was drawn while the crossings with the course runs determine the critical load factors (for T4–T66 $DLF = 1.4$). Minor increase in $DLF$ was observed for T66 ($DLF = 1.47$).

From another point of view, the maximum UY deflections in all nodes in the characteristic instant were analysed. In the DLF range of 0.8–1.2 (Fig. 14), these were of the same order of magnitude as for the characteristic node. This implicates, that the response of the structure is stable.

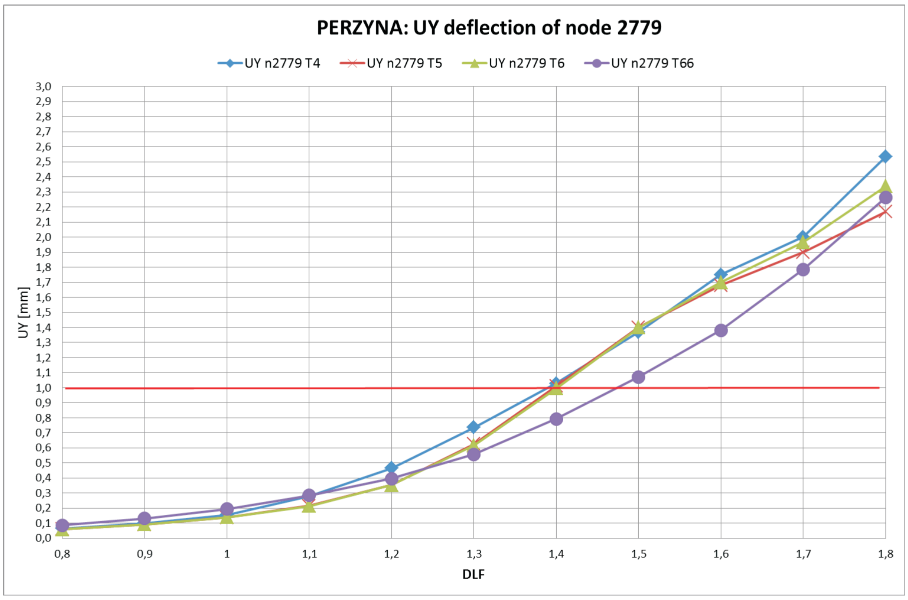


**Figure 12** UY translation (node 2779) analysis for aluminium 6060 Temper T4–T66

Analysing the results, in B–H criterion rules, similar conclusions as above can be submitted. The critical point for types T4–T6 is the vicinity of $DLF = 1.2$ when the visible change in course run is observed. The T66 tends to be more conservative, the deflection increased steadily until $DLF = 1.4$. When taking into account Volmir criterion again, the same results are achieved i.e. for T4–T6 $DLF = 1.4$ and for $T66 = 1.47$. The structure deformations of the T4 aluminium profile for $DLF = 1.4$ and $DLF = 2.6$ are presented in Fig. 13.

a) b)

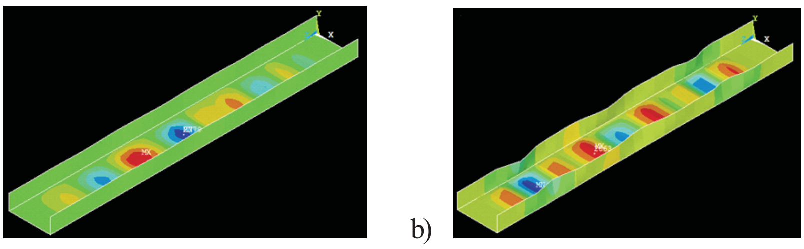

**Figure 13** Dynamic buckling mode of the T4 C–profile a) $DLF = 1.4$ and b) $DLF = 2.6$

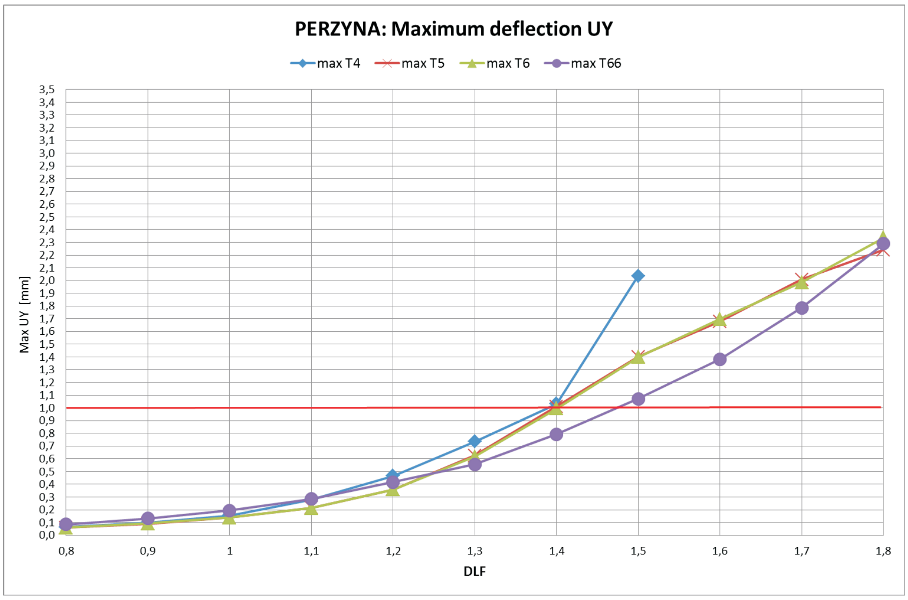


**Figure 14** Max. UY translation analysis for aluminium alloy 6060 temper T4–T66

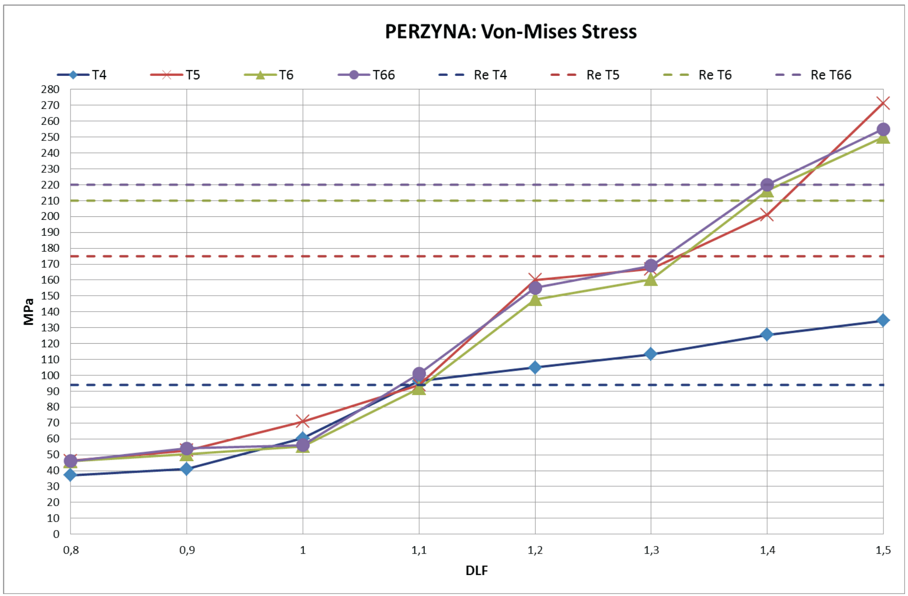


**Figure 15** Von–Misses Stress analysis for aluminium alloy 6060

In order to consider Petry–Fahlbush criterion, the Huber–Mises Stress analysis was carried out (Fig. 15). Analysing the stress ratio for all tempers, the consilience with Budiansky–Hutchinson can be observed. As the reference stress value, the yield stress was assumed. For T4; T5; T6; T66 its value was reached for $DLF = 1.1$; 1.3; 1.4 and 1.4 respectively.

**Table 1** Result summary for aluminium alloy 6060 tempers T4–T66 for modified and non–modified material characteristics

| | | | |
|---|---|---|---|
| **PERZYNA** | | | |
| **Criterion Budiansky–Hutchinson** | | | |
| UY node 2779 | Change vs. 6060 T4 UY node 2779 | max UY | Change vs. 6060 T4 max UY |
| **T4 PERZYNA (T4P)** | | | |
| 1,2 | | 1,2 | |
| **T5 PERZYNA (T5P)** | | | |
| 1,2 | 0% | 1,2 | 0% |
| **T6 PERZYNA (T6P)** | | | |
| 1,2 | 0% | 1,2 | 0% |
| **T66 PERZYNA (T66P)** | | | |
| 1,4 | 17% | 1,4 | 17% |
| **Criterion Volmir** | | | |
| UY node 2779 | Change vs. 6060 T4 UY node 2779 | max UY | Change vs. 6060 T4 max UY |
| **T4 PERZYNA (T4P)** | | | |
| 1,4 | | 1,4 | |
| **T5 PERZYNA (T5P)** | | | |
| 1,4 | 0% | 1,4 | 0% |
| **T6 PERZYNA (T6P)** | | | |
| 1,4 | 0% | 1,4 | 0% |
| **T66 PERZYNA (T66P)** | | | |
| 1,47 | 6% | 1,47 | 6% |
| **Criterion Petry–Fahlbush** | | | |
| Von–Mises Stress | | Von–Mises Stress Change vs. 6060 T4 | |
| **T4 PERZYNA (T4P)** | | | |
| 1,1 | | | |
| **T5 PERZYNA (T5P)** | | | |
| 1,3 | | 9% | |
| **T6 PERZYNA (T6P)** | | | |
| 1,4 | | 27% | |
| **T66 PERZYNA (T66P)** | | | |
| 1,4 | | 27% | |

Due to the fact, that the application of Perzyna model allow to increase the yield point, it caused the moderate change in a dynamic critical load. When considering Budiansky–Hutchinson criterion for the characteristic node and maximal UY deflection in the same instant, $DLF$ value was equal to 1.2. for T4–T6. The only increase of 17% was encountered for T66 and equalled 1.4. Respecting the Volmir criterion, the similar increase achieved 6%. Considering Petry–Fahlbush criterion, the 9%, 27%, 27% growth of $DLF$ value, for T5, T6 T66 versus T4 was noted respectively. These results were presented in the following Tab. 1.

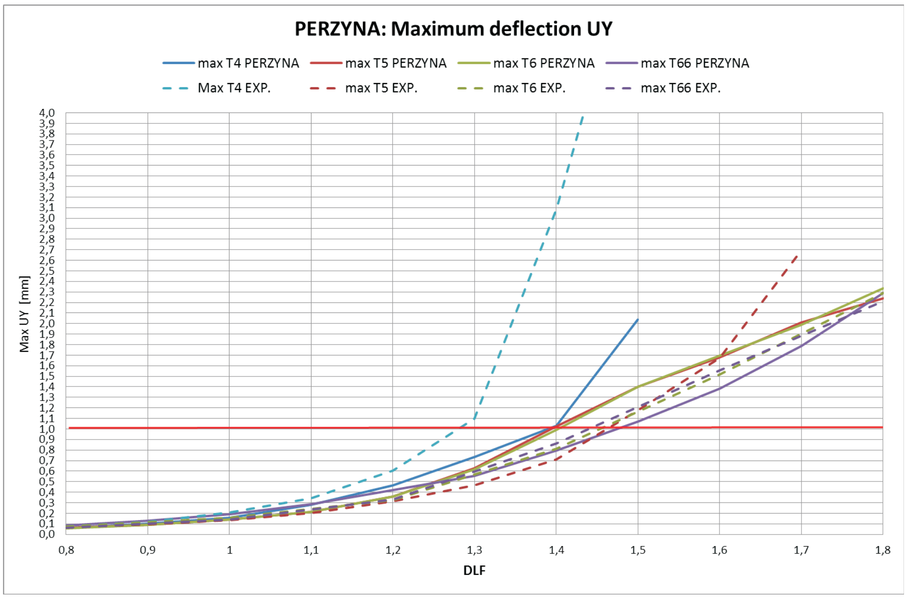


**Figure 16** Comparison od maximum UY deflection for experimental (max T_EXP.) and modified by Perzyna (max T_PERZYNA) equation material characteristics

In comparison to the results achieved in [1], when considering the viscoplasticity effect during dynamic loading, no vital difference is noticed when considering maximum UY deflections (presented in Fig. 16). The tempers T4–T6 exhibit high agreement and minor increase in stability is observed for T66. By the use of Perzyna model and consequently the elevation of yield stress limit in material characteristic, the deflections increase insignificantly but are highly repeatable independently from heat treatment type. This causes the predictable response of the structure and decreased sensitiveness to initially applied material characteristics.

Analysing the stress ratio (presented in Fig. 17), steady increase in stress is observed in the whole specified range for T5–T66. The profile made of softer T4 temper exhibits correlation to other alloy types until $DLF = 1.1$. In comparison to experimental characteristics, the courses represent higher stress tension what can be connected with higher magnitude of local deformations.

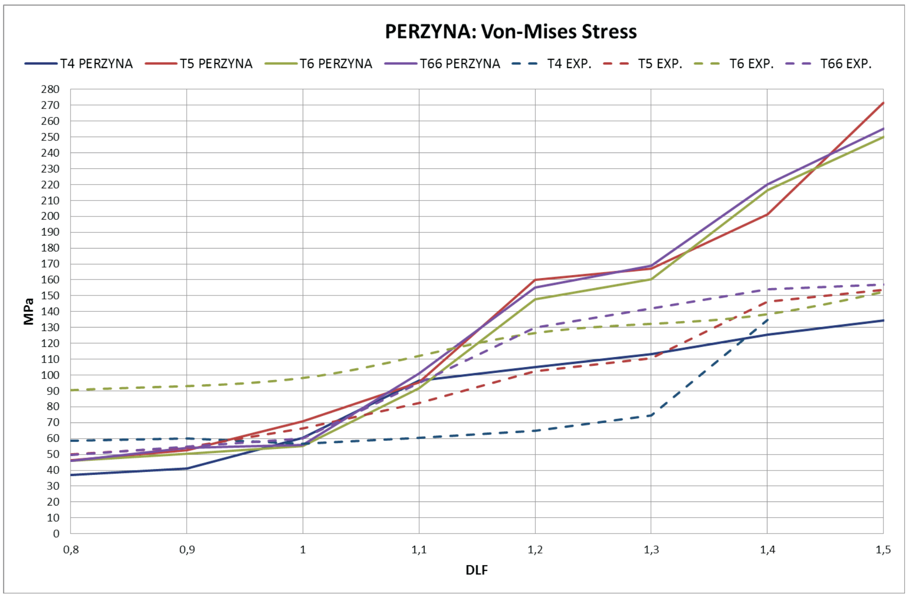


**Figure 17** Comparison of Von–Mises stress for experimental (T_EXP.) and modified by Perzyna equation (T_PERZYNA) material characteristics

Summarizing, higher deformations and Von–Mises stress rate is observed when applying Perzyna viscoplastic model. This phenomenon is compatible with experimental observations cited in the literature, that magnesium aluminium alloys exhibit lower stability on dynamic loads than observed in static or quasi–static tests. On the other hand, reproducibility of dynamic response e.g. in T5–T66 modes may lead to conclusion, that Perzyna viscoplasticity model is highly conservative and do not explicitly provide for material characteristics of the same, differently heat treated material.

## 9. Conclusion

It is evident, that members made of materials with Perzyna viscoplastic properties tend to be more conservative to dynamic buckling ratios (what is compliant with R. Mania conclusions in [23]), however are more resistant to plastic deformations. Comparing the structural response in higher range $DLF > 2,0$ with those characterized by realistic material properties, the deflections are steady growing, in vicinity of the characteristic node which is in contrast to non–modified characteristics. The example is given in Fig. 18:

The modification of material characteristics by Perzyna equations causes the elevation of yield strength but do not increase the critical value of the dynamic load factor significantly. The results for realistic material properties are more spectacular, however it is strongly recommended to verify these conclusions by experimental dynamic tests.

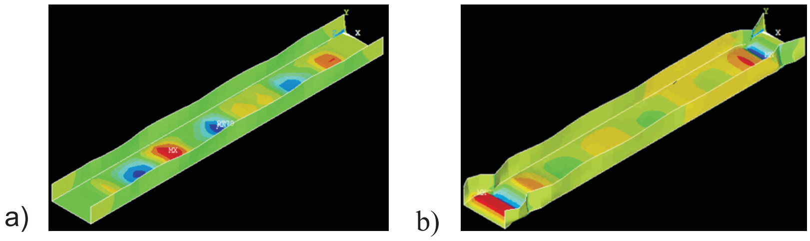

**Figure 18** The structural failure form for DLF=2.6 T66 for Perzyna Model (a) and experimental characteristic (b)

To cite the author [1], from technological point of view, the heat treatment of aluminium seems to be an alternative way to control the strength of the members and can be the only way to avoid changing of the weight and cross section of the profile when these are highly limited e.g. in air–vessels and automotive constructions applications. It is intriguing to put the step forward and invent aluminium–based, heat treated composite to upgrade the order of magnitude of dynamic load and thereby increase the dynamic critical DLF value.

## References

[1] **Mróz A. and Mania, R.**: The complex influence of aluminium aging on the dynamic response of thin walled AL 6060 alloy profile, *Thin–Walled Structures*, Vol. 79, pp. 147–153, *2014*.

[2] **Betten, J.**: Creep mechanics, 2nd Edition, *Springer–Verlag*, Berlin, Germany, **2005**.

[3] **Królak, M.**: Load carrying capacity of thin walled plated structures, in Polish, *PKN*, Warsaw–Lodz, **1990**.

[4] **Królak, M.**: Buckling, postbuckling and load carrying capacity of thin–walled orthotropic structures, monographs in Polish, *Technical University of Lodz*, **1995**.

[5] **Kowal–Michalska, K.**: The post–buckling behavior in the elasto–plastic range and ultimate strength of orthotropic plates under compression, in Polish, *Scientific Bulletin of Technical University of Lodz*, No. 721, **1995**.

[6] **Lof, J.**: Elasto–viscoplastic FEM simulations of the aluminium flow in the bearing area for extrusion of thin–walled sections, *Journal of Materials Processing Technology*, Elsevier, **2001**.

[7] **Martinez, R., Russier, W., Couzinie, J.P., Guillot, I. and Cailletaub, G.**: Modelling of the influence of coarsening on viscoplastic behavior of a 319 foundry aluminum alloy, *Materials Science & Engineering A*, Elsevier, **2013**.

[8] **Shahani, A.R., Nodamaie, S.A. and Salehinia, I.**: Parametric study on hot rolling process by the finite element method, *Mechanical Engineering*, Sharif University of Technology, Vol. 16, No. 2, **2009**.

[9] **Prager, W.**: Introduction to mechanics of continua, *Dover Publications Inc.*, Mineola, New York, **1961**.

[10] **Perzyna, P.**: The constitutive equations for rate-sensitive plastic materials, *Quart. Appl. Math.*, 20, pp. 321–332, **1963**.

[11] **Perzyna, P.** Fundamental Problems in Viscoplasticity, *Academic Press*, New York, vol. 9, pp. 243–377, *1966*.

[12] **Duvaut, G. and Lions, J. L.**: Les Inequations en mechanique et en physique, Dunod, Paris, France, **1972**.

[13] **Wang, W. M., Sluys, L. J. and de Borst, R.**: Viscoplasticity for instabilities due to strain softening and strain rate softening, *International Journal of Numerical Methods in Engineering*, 40, pp. 3839–3864, **1997**.

[14] **Wang, W. M.**: Stationary and propagative instabilities in metals: a computational point of view, Ph.D. thesis, *Delft University of Technology*, **1997**.

[15] **Łodygowski, T. and Sumelka, W.**: Future perspectives for the Perzyna's theory, 8th German–Greek–Polish Symposium, *Recent Advances in Mechanics*, Goslar, Germany, **2013**.

[16] **Astanin, V. V.**: Eksperimentalnoe isledovanie udarnowo szatia metalom v plasticeskich volnach nagruzenii intensivnostiu do 10000 MPa, *Zavodskaja Laboratoria*, **1980**.

[17] **Astanin, V. V.**: Vysokosjorostnoje deformirowanie metalov, *Zavodskaja laboratoria*, **1989**.

[18] **Zhao, H. and Gary, G.**: The testing and behavior modeling of sheey metals at strain rates from 10-4 to 104 s-1, *Materials and Science Engineering*, **1997**.

[19] **Zhang, J., Zhang, Z., Bie, J., Zhou, L. and Chen, J.**: Effect of viscosity on material behavior in friction stir welding process, *Tran. Nonferrus Met. Soc.*, China, **2006**.

[20] **Simitses, J. G.**: Dynamic stability of suddenly loaded structures, *Springer–Verlag*, New York, **1990**.

[21] **Wei, Z. G., Ju, J.I. and Batra R.C.**: Dynamic buckling of thin cylindrical shell under axial impact, *International Journal of Impact Engineering*, **2005**.

[22] **Wei, Z. G. and Batra R. C.**: Dynamic buckling of thin thermoviscoplastic cylindrical shell under radial impulsive loading, *Thin–Walled Structures*, **2006**.

[23] **Mania, R.**: Dynamic buckling of thin–walled columns made of viscoplastic materials, *Technical University of Lodz Academic Press*, **2010**.

[24] **Mukai, T., Ishikawa, K. and Higashi, K.**: Influence of strain rate on the mechanical properties in fine–grained aluminium alloys *Materials Science and Engineering*, A, 204, **1995**.

[25] **Kowal–Michalska, K.**: Dynamic Stability of Composite Plate Structures, (in Polish), *WNT*, Warszawa, **2007**.

[26] **Mróz, A.**: The influence of cross–section shape of the car roof rail on the quasi–dynamic buckling modes, in: Kowal–Michalska, K. and Mania, R.J. [eds.], *The Stability of Structures XIIIth Symposium Proceedings*, Zakopane, http://cybra.lodz.pl/publication/6250, **2012**.

[27] **Budiansky, B. and Hutchinson, J. W.**: Dynamic buckling of imperfection sensitive structures, *Proc. llrh hf. estimates. /AA J.*, 4(3), 525–530, **1966**.

[28] **Ari–Gur, J. and Elishakoff, I.**: Dynamic instability of a transversely isotropic column subjected to a compression pulse, *Computers & Structures*, Vol. 62, No. 5. pp. 815, **1997**.

[29] **Kowal–Michalska, K.**: About Some Important Parameters in Dynamic Buckling Analysis of Plated Structures Subjected to Pulse Loading, *Mechanics and Mechanical Engineering*, Vol. 14, No. 2, **2010**.

[30] **Kubiak, T.**: Criteria of dynamic buckling estimation of thin–walled structures, *Thin–walled structures*, Vol. 45, **2007**.

[31] **Hutchinson, J. W. and Budiansky, B.**: Dynamic buckling estimates, *AIAA Journal*, **1966**.

[32] **Mania, R.**: Dynamic buckling of thin–walled viscoplastic columns, *Thin–walled Structures*, **2010**.

[33] *Ansys User Guide*.